Chemistry–A European Journal

Research Article
doi.org/10.1002/chem.202103999

Chemistry Europe
European Chemical Societies Publishing

www.chemeurj.org

Gas Phase Preparation of the Elusive Monobridged Ge(μ-H)GeH Molecule through Nonadiabatic Reaction Dynamics

Zhenghai Yang[+],[a] Bing-Jian Sun[+],[b] Chao He,[a] Siti Fatimah,[b] Agnes H. H. Chang,*[b] and Ralf I. Kaiser*[a]

Abstract: The hitherto elusive monobridged Ge(μ-H)GeH (X^1A') molecule was prepared in the gas phase by bimolecular reaction of atomic germanium with germane (GeH_4). Electronic structure calculations revealed that this reaction commenced on the triplet surface with the formation of a van der Waals complex, followed by insertion of germanium into a germanium-hydrogen bond over a submerged barrier to form the triplet digermanylidene intermediate ($HGeGeH_3$); the latter underwent intersystem crossing from the triplet to the singlet surface. On the singlet surface, $HGeGeH_3$ predominantly isomerized through two successive hydrogen shifts prior to unimolecular decomposition to Ge(μ-H)GeH isomer, which is in equilibrium with the vinylidene-type (H_2GeGe) and dibridged (Ge(μ-H_2)Ge) isomers. This reaction leads to the formation of cyclic dinuclear germanium molecules, which do not exist on the isovalent C_2H_2 surface, thus deepening our understanding of the role of nonadiabatic reaction dynamics in preparing nonclassical, hydrogen-bridged isomers carrying main group XIV elements.

Introduction.

Despite sharing the same number of valence electrons, the chemical bonding and structures of silicon- and germanium-bearing compounds differ strongly from those of their carbon counterparts leading to new views on the concept of isoelectronicity.[1] Four structural isomers of Ge_2H_2 were located computationally on the ground-state singlet surface; these include a doubly bridged butterfly structure (Ge(μ-H_2)Ge; **7**), a *cis* monobridged form (Ge(μ-H)GeH; **8**), a vinylidene-type isomer (H_2GeGe; **9**), and a *trans*-bent form (HGeGeH; **10**; Scheme 1). Among these four isomers, the butterfly structure, **7**, in which both germanium atoms are connected by a σ-bond with the hydrogen atoms attached to the heavy atoms by three-center-two-electron (**3c**–**2e**) bonds, is the thermodynamically most stable Ge_2H_2 isomer with the *cis* monobridged structure, **8**, being the second most stable isomer.[2]

The vinylidene-type digermenylidene structure **9** is predicted to lie 9 kJ mol^{-1} above *cis* monobridged Ge(μ-H)GeH. The structures and relative stabilities of these Ge_2H_2 isomers reveal overall similarity to the Si_2H_2 system (**3**–**6**).[3] However, carbon analogues of the hydrogen-bridged equilibrium structures Ge-(μ-H_2)Ge (**7**) and Ge(μ-H)GeH (**8**) do not exist; the linear acetylene molecule **1** is the lowest-lying isomer in the C_2H_2 system.[4] The existence of unusual, nonclassical hydrogen bridged equilibrium structures in the Ge_2H_2 system can be explained by interaction between two GeH moieties resulting into a dibridged structure.[2c,5] Moreover, the length of the Ge–Ge double bond in digermylidene **9** is longer than the

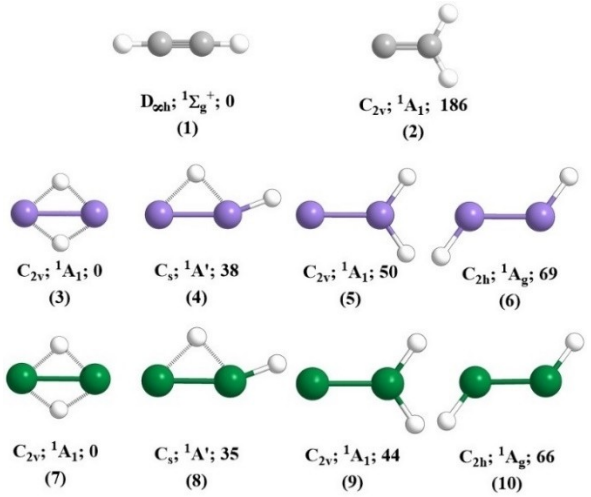

Scheme 1. Structures, point groups, electronic states, and relative energies [kJ mol^{-1}] of homonuclear dihydrides: C_2H_2 (**1**, **2**), Si_2H_2 (**3**–**6**), and Ge_2H_2 (**7**–**10**). Atoms are color coded in green (germanium), purple (silicon), gray (carbon), and white (hydrogen).

[a] Dr. Z. Yang,[+] Dr. C. He, Prof. Dr. R. I. Kaiser
Department of Chemistry
University of Hawai'i at Manoa
Honolulu, Hawaii 96822 (USA)
E-mail: ralfk@hawaii.edu

[b] Dr. B.-J. Sun,[+] Dr. S. Fatimah, Prof. Dr. A. H. H. Chang
Department of Chemistry
National Dong Hwa University
Shoufeng, Hualien 974 (Taiwan)
E-mail: hhchang@gms.ndhu.edu.tw

[+] These authors contributed equally to this work.

Supporting information for this article is available on the WWW under https://doi.org/10.1002/chem.202103999

© 2021 Wiley-VCH GmbH

trans-bent bond values in digermene (H_2GeGeH_2);[6] this contrasts with the carbon analog structures, where the ethylene isomer holds the longer C–C bond distance of 1.339 Å compared to 1.316 Å.[7] This can be rationalized by the fact that the bonds of Ge_2H_2 are polarized strongly toward the more electronegative hydrogen atoms resulting in a less effective hyperconjugation.[6a]

Homo- and heteronuclear dihydrides of main group XIV have been the subject of extensive experimental attention. Among the $SiCH_2$ isomers, the simplest unsaturated silylene (H_2CSi) represents the global minima and was first identified in 1979 by flash photolysis of a mixture of methylsilanes and helium.[8] Subsequently, this isomer was explored by laser-induced fluorescence (LIF) along with wavelength-resolved fluorescence and stimulated emission pumping (SEP).[9] In 2008, the H_2CSi isomer was also proposed to be prepared under single collision conditions.[10] Considering the $GeCH_2$ system, germavinylidene (H_2CGe), the lowest lying isomer and the simplest unsaturated germylene, was identified experimentally as well. The first laser spectroscopic detection of germavinylidene was reported in 1997;[9b] a series of follow up experimental studies were conducted investigating both ground and excited electronic states of germavinylidene.[11] These studies verified the reduced overlap of the valence s and p orbitals of the heavy main group XIV elements as compared to carbon.[12] Recently, two crossed molecular beam studies involving the simplest open-shell species and the prototype closed shell molecules of atomic germanium with silane and of atomic silicon with germane shed light on the hetero-nuclear $SiGeH_2$ system.[13] In both systems, the thermodynamically most stable $SiGeH_2$ isomer, the doubly bridged butterfly structure (Si(μ-H_2)Ge), was prepared in the gas phase. As for the Si_2H_2 analogs, the butterfly structure **3**[14] and the *cis* monobridged isomer **4**[15] have been prepared as well; a gas-phase crossed beam study also revealed the formation of the vinylidene-type disilavinylidene isomer **5**.[3] However, compared to the isovalent systems, the Ge_2H_2 system has received little attention despite the potential to explore unusual, hydrogen-bridged molecules. Until recently, only the dibridged Ge(μ-H_2)Ge isomer (**7**) has been detected experimentally by matrix isolation coupled with infrared spectroscopy, but no gas-phase studies have been explored to prepare distinct Ge_2H_2 isomers under single collision conditions.[16]

Here, we report the *directed* gas-phase preparation of the previously elusive monobridged Ge(μ-H)GeH isomer **8** by exploiting a crossed molecular beam machine through bimolecular reactions of ground-state open-shell atomic germanium (Ge; ^3P_j) with closed-shell germane (GeH_4; X^1A_1). By merging experimental results with electronic structure and statistical calculations, the unusual structures and exotic chemical bonding of dinuclear germanium compounds is revealed. The reaction is predicted to be initiated on the triplet surface with the formation of a van der Waals complex, followed by insertion of germanium into germanium-hydrogen bond with a submerged barrier and intersystem crossing (ISC) from the triplet to the singlet surface thus deepening our understanding of the non-adiabatic reaction dynamics in dinuclear systems of various degrees of hydrogenation incorporating main group 14 elements.

Results and Discussion

Laboratory frame

The reactive scattering signal of the reaction of germanium (Ge; ^3P_j) with germane (GeH_4; X^1A_1) was probed from mass-to-charge (*m/z*) 156 ($^{76}Ge_2H_4^+$) to 140 ($^{70}Ge_2^+$) accounting for the natural isotope abundances of germanium [^{70}Ge (20.5 %), ^{72}Ge (27.4 %), ^{73}Ge (7.8 %), ^{74}Ge (36.7 %), ^{76}Ge (7.8 %)]. No definite signal could be detected from *m/z* 153 to 156, thus suggesting that no Ge_2H_4 adducts were produced. The signal at *m/z* 150 ($^{73}Ge^{74}GeH_3^+$/$^{74}Ge_2H_2^+$/$^{72}Ge^{76}GeH_2^+$/$^{73}Ge^{76}GeH^+$/$^{74}Ge^{76}Ge^+$) was found to depict the best signal-to-noise ratio (Table S2 in the Supporting Information) with TOFs at the remaining *m/z* ratios superimposable after scaling. These findings suggest that the Ge–GeH_4 reaction proceeds through a single reaction channel, that is, a molecular hydrogen loss channel forming $^{74}Ge_2H_2$ (150 amu) along with molecular hydrogen (2 amu; reaction 2). The Ge + GeH_4→2 GeH_2 channel leading to the formation of GeH_2 radical is closed under our experimental conditions considering the endoergicity of 39 kJ mol^{-1} (Supporting Information). Ion counts collected at *m/z* 140–149 originate from dissociative electron impact ionization of the $^{74}Ge_2H_2$ (*m/z* 150) parent along with the isotopically substituted counterparts. Note that the atomic hydrogen loss channel leading to the formation of any Ge_2H_3 isomers (reaction 1) is endoergic by at least 118 kJ mol^{-1} and is therefore closed considering our collision energy of 24.3 ± 0.4 kJ mol^{-1}.[17] The angular resolved TOF spectra were therefore collected in 2.5° intervals at *m/z* 150 ($^{74}Ge_2H_2^+$) and scaled to the TOF taken at the CM angle yielding the laboratory angular distribution (LAD).

The LAD spread over 35° and is nearly forward-backward symmetric with respect to the CM angle, also holds a maximum at the CM angle (Figure 1). These findings suggests that the Ge–GeH_4 reaction likely involves indirect reaction dynamics involving the formation of Ge_2H_4 intermediates.[18]

$$Ge + GeH_4 \rightarrow Ge_2H_3\ (151\,amu) + H\ (1\,amu) \quad (1)$$

$$Ge + GeH_4 \rightarrow Ge_2H_2\ (150\,amu) + H_2\ (2\,amu) \quad (2)$$

Center-of-mass frame

Although the laboratory data alone identify the germanium versus molecular hydrogen pathway, the nature of the Ge_2H_2 product isomer(s) and the underlying reaction mechanism(s) have to be exposed.

This information can be derived by transforming the laboratory data into the CM reference frame.[19] The laboratory data were fit with a single channel, that is, a molecular hydrogen loss channel with a mass combination of 150 amu

© 2021 Wiley-VCH GmbH

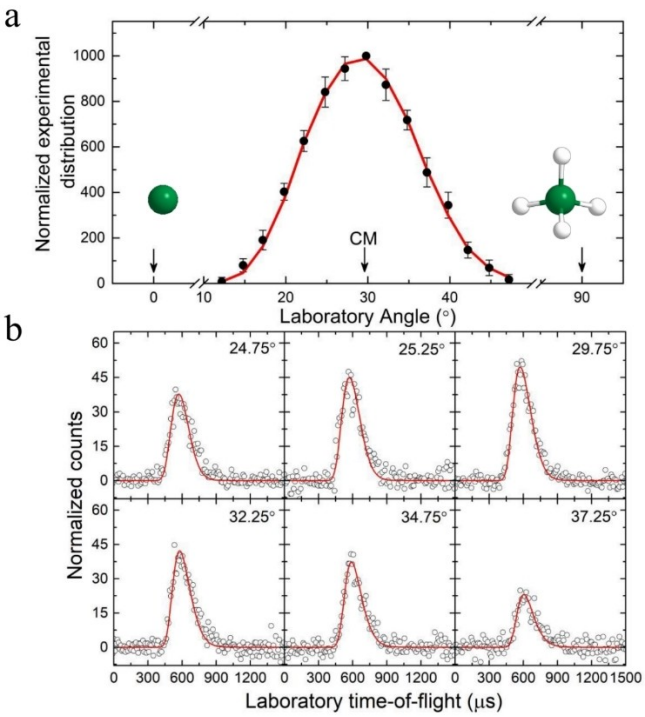

Figure 1. a) Laboratory angular distribution and b) time-of-flight spectra collected at *m/z* 150 ($^{74}Ge_2H_2^+$) in the reaction of ground-state atomic germanium with germane. The circles represent the experimental results, and the red lines depict the best fits.

($^{74}Ge_2H_2$, hereafter Ge_2H_2) plus 2 amu (H_2). The best fit CM translational energy $P(E_T)$ and angular $T(\theta)$ flux distributions are depicted in Figure 2. Inspecting the $P(E_T)$ distribution, the maximum translational energy E_{max} of 108 ± 18 kJ mol^{-1} characterizes the sum of the collision energy (24.3 ± 0.4 kJ mol^{-1}) and the reaction exoergicity for those products formed without internal excitation. Hence, the experimental reaction energy is suggested to be -84 ± 18 kJ mol^{-1}. However, considering that germanium was produced in the $j=0$, 1, and 2 states with $j=1$ and 2 higher in energy by 7 and 17 kJ mol^{-1} than $j=0$, the aforementioned energy of -84 ± 18 kJ mol^{-1} has to be reduced by 17 kJ mol^{-1} to reveal the true reaction energy to be -67 ± 18 kJ mol^{-1}. Furthermore, the off-zero peaking of the $P(E_T)$ distribution (26 ± 4 kJ mol^{-1}) indicates a tight-exit transition state forming Ge_2H_2 plus molecular hydrogen. Finally, the forward-backward symmetric $T(\theta)$ distribution shows non-zero intensity from 0° to 180°, thus implying indirect scattering dynamics via long-lived (lifetime longer than the rotational period) Ge_2H_4 complex(es).[18,20]

Discussion

In the case of complex potential energy surfaces (PES), It is always beneficial to merge the experimental data with electronic structure calculations. Our calculations identified nine Ge_2H_2 product isomers on the singlet (**p1**–**p4**) and triplet surface (^{3}**p1**–^{3}**p3**, *trans/cis*-^{3}**p4**). On the singlet surface, the dibridged di-μ-hydrodigermanium butterfly molecule (**p1**, -105 ± 7 kJ mol^{-1}, Ge(μ-H_2)Ge, C_{2v}, X^1A_1) represents the thermodynamically most stable isomer followed by a monobridged isomer (**p2**, -70 ± 7 kJ mol^{-1}, Ge(μ-H)GeH, C_s, X^1A'), digermenylidene (**p3**, -61 ± 7 kJ mol^{-1}, H_2GeGe, C_{2v}, X^1A_1), and singlet *trans*-bent digermyne (**p4**, -39 ± 7 kJ mol^{-1}, HGeGeH, C_{2h}, X^1A_g). The computed relative energies of these products agree very well with the previous results.[2a,b,6b] The triplet structures are consistently higher in energy than their singlet counterparts: triplet digermenylidene (^{3}**p3**, -17 ± 7 kJ mol^{-1}, H_2GeGe, C_{2v}, a^3A_2), triplet *trans*-bent digermyne (*trans*-^{3}**p4**, -11 ± 7 kJ mol^{-1}, HGeGeH, C_{2h}, a^3A_u), triplet *cis* digermyne (*cis*-^{3}**p4**, 17 ± 7 kJ mol^{-1}, HGeGeH, C_s, a^3A''), triplet monobridged isomer (^{3}**p2**, $22 \pm$

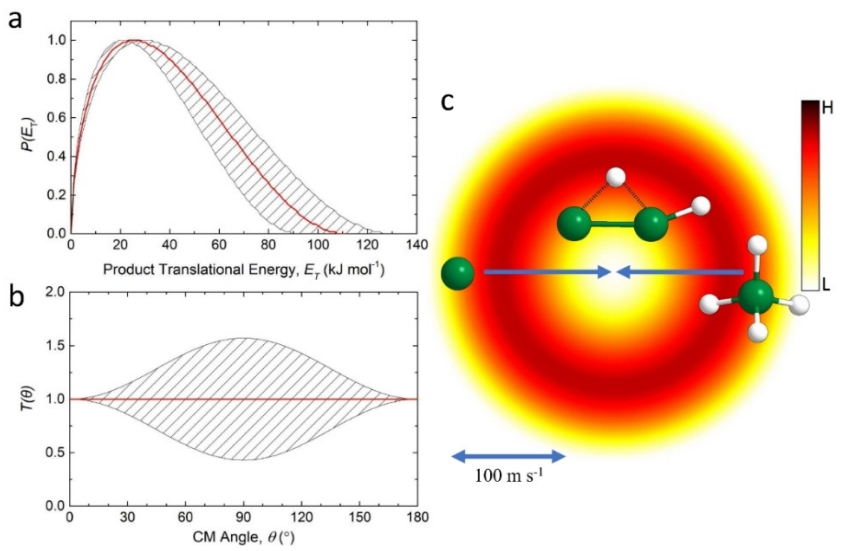

Figure 2. a) CM translational energy, b) angular flux distributions and c) the associated flux contour map for the reaction of atomic germanium with germane forming Ge_2H_2 isomer(s) through molecular hydrogen elimination. The red lines indicate the best-fit; shaded areas represent the error limits.

© 2021 Wiley-VCH GmbH

7 kJ mol^{-1}, Ge(μ-H)GeH, C_1, a^{3}A), and triplet dibridged butterfly molecule (^{3}**p1**, 64 ± 7 kJ mol^{-1}, Ge(μ-H$_2$)Ge, C_s, a^{3}A′′). A comparison of the experimentally determined reaction energy of −67 ± 18 kJ mol^{-1} with the computed data suggest that for those molecules born without internal excitation, at least the monobridged isomer (**p2**, −70 ± 7 kJ mol^{-1}, Ge(μ-H)GeH, C_s, X^{1}A′) represents a viable product on the singlet surface. Considering that the reaction starts on the triplet surface, but both products are formed in their singlet ground state, nonadiabatic reaction dynamics drive the outcome of the bimolecular gas-phase reaction of atomic germanium with germane. Note that singlet **p3** and **p4** cannot be excluded at the present stage since their contributions might be hidden in the low energy section of the *P(E$_T$)*. It is important to note that on the triplet surface, the formation of ^{3}**p1** and ^{3}**p2** is endoergic; these endoergicities cannot be compensated by the collision energy of 24.3 ± 0.4 kJ mol^{-1}. Nevertheless, based on the energetics alone, ^{3}**p3** and ^{3}**p4** might contribute to reactive scattering signal.

Based on these findings, both the triplet and singlet Ge_2H_4 PESs along with intersystem crossing (ISC) from the triplet to the singlet manifold are explored (Figures 3 and S1). The computations predict that the atomic germanium (^{3}P$_0$)-germane (X^{1}A$_1$) reaction is initiated on the triplet surface through a de-facto barrierless insertion of germanium into one of the germanium-hydrogen bonds of germane. When the ground-state germanium atom approaches the germane molecule, the PES is attractive resulting in a van der Waals (vdW) complex bound by 30 kJ mol^{-1} relative to the separated reactants. Through insertion of the germanium atom into the germane germanium – hydrogen bond, the vdW complex can isomerize to the covalently bound intermediate ^{3}**i1** (HGeGeH$_3$, digermanylidene, C_s, ^{3}A′′) over a barrier of 25 kJ mol^{-1}. It is important to stress that the overall reaction from the separated reactants to ^{3}**i1** is still barrierless since the vdW complex and ^{3}**i1** are connected via a transition state located 5 kJ mol^{-1} *below* the separated reactants, that is, a submerged barrier.[21] ^{3}**i1** can emit molecular hydrogen forming triplet ^{3}**p3** and *trans*-^{3}**p4**, or isomerize to ^{3}**i3** (H$_2$GeGeH$_2$; digermene, C_1, ^{3}A) through a hydrogen shift followed by molecular hydrogen emission leading to ^{3}**p3** and ^{3}**p4**. However, the transition states connecting ^{3}**i1** to ^{3}**p3** and *trans*-^{3}**p4** and ^{3}**i3** are located 49, 96 and 29 kJ mol^{-1} above the separated reactants respectively; thus these pathways should be closed considering our collision energy of 24.3 ± 0.4 kJ mol^{-1}. Based on these considerations, no triplet Ge_2H_2 isomers can be formed in the Ge–GeH$_4$ reaction since the tight-exit transition states cannot be surpassed energetically under our experimental conditions.

How are the singlet Ge_2H_2 product isomers formed? The calculations predict the possibility of ISC from the triplet to singlet manifolds. In detail, intermediate ^{3}**i1** undergoes ISC to intermediate **i1** (HGeGeH$_3$; digermanylidene, C_s, ^{1}A′), which lies 75 kJ mol^{-1} below ^{3}**i1**. The seam of crossing (MSX) residing 89 kJ mol^{-1} below the separated reactants is identified with a similar geometry to that of ^{3}**i1**.

One notable difference between ^{3}**i1** and MSX is the change of the H–Ge–Ge angle, that is, an increase from 122.6° in ^{3}**i1** to 126.9° in MSX. On the singlet surface, intermediate **i1** can undergo unimolecular decomposition to **p3**, but the tight transition state connecting **i1** and **p3** is located 63 kJ mol^{-1} above the separated reactants and cannot be overcome under our experimental conditions considering a collision energy of

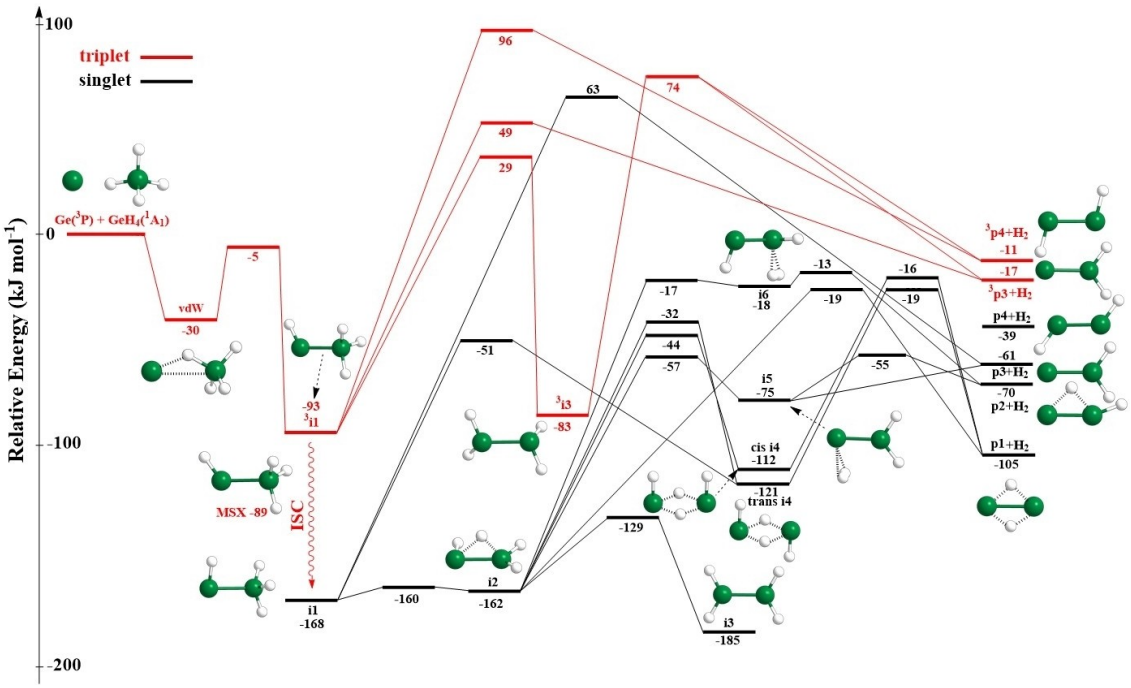

Figure 3. Potential energy surface (PES) for the reaction of the atomic germanium with germane. A complete PES is presented in Figure S1 (Supporting Information). Germanium and hydrogen atoms are color coded in green and white, respectively.

© 2021 Wiley-VCH GmbH

only 24.3 ± 0.4 kJ mol^{-1}. Alternatively, **i1** can undergo isomerization yielding dibridged *trans*-HGe(μ-H$_2$)GeH intermediate *trans*-**i4** (C_{2h}, X^{1}A$_g$) via a transition-state located 117 kJ mol^{-1} above **i1** or may isomerize to the monobridged structure **i2** (H$_2$Ge(μ-H)GeH, C$_1$, X^{1}A) with a barrier of 8 kJ mol^{-1}. Considering the isomerization barriers, the formation of **i2** is suggested to be preferred. What's the fate of **i2**? Our computations reveal that six energetically accessible channels are open: i) isomerization to **i6** (C$_1$, X^{1}A) via a transition state located 145 kJ mol^{-1} above **i2**, ii) unimolecular decomposition to **p1** through a transition state located 143 kJ mol^{-1} above **i2**, iii) formation of intermediate *trans*-**i4** through hydrogen atom migration and a barrier of 130 kJ mol^{-1}, iv) hydrogen atom migration leading to a dibridged structure, *cis*-HGe(μ-H$_2$)GeH (*cis*-**i4**, C_{2v}, ^{1}A$_1$) via a transition state residing 118 kJ mol^{-1} above **i2**, v) isomerization to **i5** (C$_s$, X^{1}A′) by passing a transition state 57 kJ mol^{-1} below the reactants and 105 kJ mol^{-1} above **i2**, and vi) isomerization to **i3**. However, our calculations identified that **i3** can eliminate molecular hydrogen to **p3** only according to **i3**→**i2**→**i5**→**p3** + H$_2$ pathway. The barriers might suggest that the formation of **i5** is favored considering the transition states to isomerization (**i3**→**i2**→**i5**, **i2**→**i5** vs. **i2**→*cis*-**i4**, **i2**→*trans*-**i4**, **i2**→**p1**, and **i2**→**i6**).

Intermediate **i5** may undergo unimolecular decomposition via tight-exit transition states to Ge(μ-H)GeH (**p2**) and/or H$_2$GeGe (**p3**) according to a barrierless pathway; the latter contradicts our experimental findings of a tight-exit transition state. **p2** can also be formed from **i6** after molecular hydrogen loss and a tight-exit transition state. Moreover, decomposition of *cis*- and *trans*-**i4** could lead to **p1**, which might represent the minor contributor in the experiment. Note that according to the calculation, if the monobridged isomer **p2** is formed with sufficient internal energy, it can isomerize to **p1** or **p3** by overcoming barriers of 13 and 18 kJ mol^{-1}, respectively (Figure 4). Therefore, although **p2** represents the initial reaction product under single collision condition, it can be in equilibrium with the isomers **p1** and **p3**. In multicollision environments, all three isomers can be stabilized by three-body collision thus making these available for spectroscopic detection by transferring (parts of) the internal energy to the three-body collider.

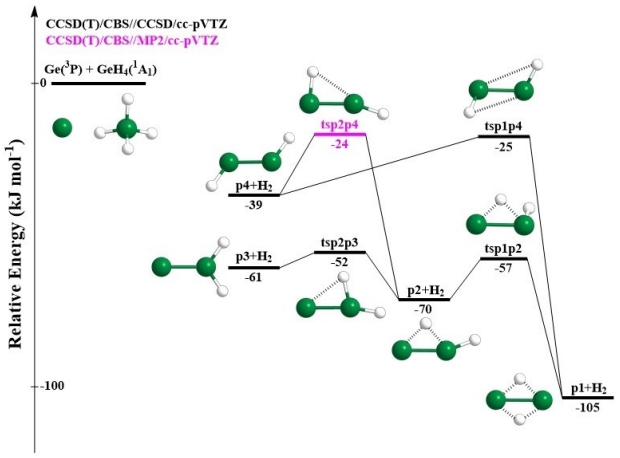

Figure 4. Relative energies of singlet products and the transition states connecting these products.

Conclusions

Overall, merging experimental findings with computational results suggests that ground-state atomic germanium reacts with germane on the triplet surface forming a van der Waals complex that isomerizes by germanium atom insertion into a germanium–hydrogen bond to ^{3}**i1**. The latter undergoes ISC to intermediate **i1** (HGeGeH$_3$; digermanylidene, C$_s$, ^{1}A′), which then undergoes a hydrogen shift to the hydrogen-bridged intermediate **i2** on the singlet surface. The latter undergoes yet another hydrogen shift to form **i5**, in which the molecule hydrogen moiety is already formed. This intermediate loses molecular hydrogen via a tight-exit transition state to form the monobridged isomer (**p2**, Ge(μ-H)GeH, C_s, X^{1}A′) in an overall exoergic reaction (theoretical: −70 ± 7 kJ mol^{-1}, experimental: −67 ± 18 kJ mol^{-1}) according to nonadiabatic reaction dynamics. These conclusions are in line with energy-dependent Rice–Ramsperger-Kassel-Marcus (RRKM) calculations (Supporting Information), which predict that **p2** is predominantly formed at a level of 91 %, with **p1** and **p3** contributing only 6 and 3 % at our collision energy of 24.3 ± 0.4 kJ mol^{-1}, thus supporting the first gas-phase identification of the previously elusive monobridged Ge(μ-H)GeH (X^{1}A′) molecule. Any **p2** formed with sufficient internal energy can isomerize to **p1** and **p3** by hydrogen shifts.

The chemical dynamics of the Ge (^{3}P)–GeH$_4$ (X^{1}A$_1$) system are quite distinct from the dynamics of the isovalent E–EH$_4$ (E=C, Si) reactions. For the carbon (C; ^{3}P)-methane (CH$_4$; ^{1}A$_1$) system, the molecular hydrogen elimination pathway to acetylene and vinylidene is closed given the inherent barrier of about 51 kJ mol^{-1} to the insertion of atomic carbon into the carbon-hydrogen bond of methane.[22] Further, carbon analogues of the unusual mono- and dibridged intermediates formed in germanium–germane reactions do not even exist. The study by Yang et al. revealed that the silicon (Si; ^{3}P)-silane (SiH$_4$; X^{1}A$_1$) reaction is initiated by the barrierless formation of a van der Waals complex that can isomerize to triplet disilamethylcarbene (HSiSiH$_3$) through insertion of the silicon into a silicon-hydrogen bond. The triplet HSiSiH$_3$ intermediate undergoes ISC to singlet HSiSiH$_3$.[3] Up to here, the reaction dynamics depict a strong analogy to the Ge (^{3}P)–GeH$_4$ (X^{1}A$_1$) system. However, singlet HSiSiH$_3$ isomerizes to a long-lived disilaethylene intermediate by a hydrogen shift and finally eliminates molecular hydrogen initially forming singlet disilavinylidene (H$_2$SiSi). The internal energy of singlet disilavinylidene (H$_2$SiSi) supports isomerization to the monobridged Si(μ-H)SiH (X^{1}A′) isomer. Overall, the insights from isovalent carbon and silicon systems are not readily leveraged to interpret isovalent gas-phase reactions of germanium. The findings of our study provide new evidence regarding the difference of the reaction dynamics of isovalent systems, especially those involving main group 14 elements. Considering that the hydrogen atoms in germane can be substituted by side groups, the extracted reaction dynamics might be helpful to predict and to eventually

© 2021 Wiley-VCH GmbH

explore the formation of the largely obscure group of substituted germanium-bearing hydrogen bridged structures on the molecular level in the gas phase.

Experimental Section

The gas-phase reaction of ground-state atomic germanium (Ge; ^{3}P) with germane (GeH_4; X^1A_1) was studied in a crossed molecular beam machine.[23] The supersonic beam of the primary reactant-atomic germanium-was generated in situ by exploiting laser ablation using 266 nm laser (Nd:YAG; 30 Hz; 3 ± 1 mJ per pulse) of a germanium rod, which was kept in helical motion (optical-grade; Alfa Aesar).[13a] The ablated germanium atoms were seeded in neon (99.9999 %; Matheson) as released by a pulsed valve operated at 60 Hz with 4 atm backing pressure. After being skimmed, the atomic germanium beam was velocity-selected by a four-slot chopper wheel operating at 120 Hz to a well-defined v_p (peak velocity) of 998 ± 12 m s^{-1} and S (speed ratio) of 5.6 ± 0.2 (Table S1). No higher germanium clusters were detected in the experiment. In the scattering chamber, the primary beam crossed a section of a pulsed molecular beam of pure germane (GeH_4; Air Liquide; 99.999 %; 60 Hz; 550 Torr) defined by $v_{p=}$529 ± 5 m s^{-1} and S = 9.0 ± 0.7 perpendicularly. The corresponding collision energy (E_c) and center of mass angle (Θ_{CM}) were then determined to be 24.3 ± 0.4 kJ mol^{-1} and 29.4 ± 0.4°, respectively, for the ^{74}Ge and $^{74}GeH_4$ reactants. Laser-induced fluorescence (LIF) reveals that atomic germanium is produced not only in the $^3P_0$ state, but also in the $^3P_1$ and $^3P_2$ states with j = 1 and 2 lying 7 and 17 kJ mol^{-1} higher in energy than j = 0.[24] The neutral reactive-scattering products were ionized utilizing an electron impact ionizer (80 eV; 2 mA) operating at ultrahigh-vacuum conditions of 6 × 10^{-12} Torr and mass filtered by a quadrupole mass spectrometer (QMS). The detection system recorded the products flight time from the interaction region via the ionizer to the Daly target in the time-of-flight (TOF) mode. The laboratory data, that is, the laboratory angular distribution (LAD) and the TOF spectra, were transformed using a forward-convolution routine from the laboratory into the CM reference frame to extract information of the reaction dynamics.[25] This approach provides the CM translational energy $P(E_T)$ and the angular $T(\theta)$ flux distributions along with the contour flux map of the product molecule, $I(u,\theta) \approx P(u) \times T(\theta)$, with the CM velocity u and angle θ. A reactive scattering cross section of an $E_T^{-1/3}$ energy dependence was utilized in the fitting procedure within the line-of-center model considering the barrierless reaction.[18,26]

Computational Methods

The H_2 loss channels of the atomic germanium (Ge, ^{3}P) and germane (GeH_4, $^1A_1$) reaction on both Ge_2H_4 adiabatic triplet and singlet ground-state potential energy surfaces are characterized. The coupled cluster[27] CCSD/cc-pVTZ calculations are employed in the optimization for the geometries of collision complexes, intermediates, transition states, and H_2 dissociation products, with the exception of **i6**, **tsi2i6**, and **tsi6p2**, which are found through MP2/cc-pVTZ. Their CCSD(T)/CBS (complete basis set limits[28]) energies with CCSD/cc-pVTZ zero-point energy corrections are obtained by extrapolating the CCSD(T)/cc-pVDZ, CCSD-(T)/cc-pVTZ, and CCSD(T)/cc-pVQZ energies, with an expected accuracy within 7 kJ mol^{-1}.[29] The 1-D CCSD(T)/CBS barrierless potential energy curve for **i5**→**p3** along the reaction coordinate is likewise evaluated at CCSD/cc-pVTZ optimized structures with CCSD/cc-pVTZ zero-point energy corrections. CPMCSCF[30]/TZVPP calculations are carried out for location of the minimum energy crossing point between ^{3}**i1** and ^{1}**i1**, with CCSD(T)/CBS energy then obtained. GAUSSIAN16 programs[31] and MOLPRO[30] programs were used for the coupled cluster and the surface-crossing computations, respectively.

On singlet potential energy surface, the RRKM rate constants[32] are computed at collision energies of 0.0, 5.0, 10.0, 20.0, 24.3, 30.0, and 40.0 kJ mol^{-1}. The density of states for the intermediates and the number of states for the transition states are evaluated by the saddle-point method[32–33] with the CCSD(T)/CBS energies and CCSD/cc-pVTZ harmonic frequencies. All species are treated as a collection of harmonic oscillators. The variational transition state (**tsi5p3**) on the barrierless potential curve is characterized by using variational RRKM theory.[34] Finally, with the aid of RRKM rate constants, the energy-dependent product branching ratio is obtained by solving the rate equations based on reaction mechanism (derived from ab initio reaction paths) using the Runge – Kutta method.

In addition to primary reactions, the secondary reactions: **p1**, **p2**, **p3**, and **p4** isomerizations are also considered at 0.0 and 24.3 kJ mol^{-1}collision energies. Presumably, only the vibrational energy in primary products, **p1**, **p2**, and **p3**, could participate in the secondary reactions. To estimate the vibrational energies of primary **p1**, **p2**, and **p3**, the theoretical energy-partition model[34c] that accounts for the statistical nature of the energy above transition state and the impulsiveness of the exit barrier is adapted. Simply, at 0.0 collision energy, the available energy ($\mathbf{E^{ava}}$) for **p2** + H_2 is 70 kJ mol^{-1} as seen in Figures 3 and 4; however only vibrational energy in **p2** would take part in secondary reactions, isomerization. The exit barrier ($\mathbf{E^{imp}}$) 15 kJ mol^{-1} (−55–(−70) kJ mol^{-1}) for **i5**→**p2** + H_2 channel contributes only to translational and rotational energies of **p2** + H_2. The energy ($\mathbf{E^{stat}}$) above the transition state (**tsi5p2**), 55 kJ mol^{-1} is partitioned among the translational, rotational, and vibrational energies of two fragments, **p2** and H_2. Thus, only the vibrational energy of **p2** contributed from $\mathbf{E^{stat}}$ would make **p2** isomerization possible, which is estimated to be 25 kJ mol^{-1}, or meaning 70 − 15 − 30 = 25 kJ mol^{-1}. (25 kJ mol^{-1} is obtained by assuming similar partitions as the H_2 loss channels of O (^{1}D) + CH_4 reaction.[35]) Among all the primary product (**p1**, **p2**, **p3**) channels, only **p2** produced from **i5**→**p2** + H_2 channel has enough vibrational energy to proceed secondary reactions. The corresponding RRKM rate constants with corrected available energies are computed. Accordingly, reaction mechanism including secondary reactions are devised to solve rate equations and obtain product branching ratios.

Acknowledgements

This work at the University of Hawaii was supported by the US National Science Foundation (CHE-1853541). The calculations were performed with computer resources at the National Center for High-Performance Computing of Taiwan.

© 2021 Wiley-VCH GmbH

Conflict of Interest

The authors declare no conflict of interest.

Data Availability Statement

The data that support the findings of this study are available from the corresponding author upon reasonable request.

Keywords: gas-phase reactions · germane · germanium · group 14 elements · reaction dynamics

[1] a) I. Langmuir, *J. Am. Chem. Soc.* **1919**, *41*, 868–934; b) I. Langmuir, *J. Am. Chem. Soc.* **1919**, *41*, 1543–1559; c) P. P. Power, *Chem. Rev.* **1999**, *99*, 3463–3504; d) R. C. Fischer, P. P. Power, *Chem. Rev.* **2010**, *110*, 3877–3923.
[2] a) R. S. Grev, B. J. Deleeuw, Y. Yamaguchi, S.-J. Kim, H. F. Schaefer III in *Structures and Conformations of Non-rigid Molecules*, Springer, 1993, pp. 325–342; b) Z. Palágyi, H. F. Schaefer III, E. Kapuy, *J. Am. Chem. Soc.* **1993**, *115*, 6901–6903; c) M. Lein, A. Krapp, G. Frenking, *J. Am. Chem. Soc.* **2005**, *127*, 6290–6299.
[3] T. Yang, B. B. Dangi, R. I. Kaiser, K. H. Chao, B. J. Sun, A. H. H. Chang, T. L. Nguyen, J. F. Stanton, *Angew. Chem. Int. Ed.* **2017**, *56*, 1264–1268; *Angew. Chem.* **2017**, *129*, 1284–1288.
[4] a) M. M. Gallo, T. P. Hamilton, H. F. Schaefer III, *J. Am. Chem. Soc.* **1990**, *112*, 8714–8719; b) H. Lee, J. H. Baraban, R. W. Field, J. F. Stanton, *J. Phys. Chem. A* **2013**, *117*, 11679–11683.
[5] K. T. Petrov, T. Veszprémi, *Int. J. Quantum Chem.* **2009**, *109*, 2526–2541.
[6] a) R. S. Grev, B. J. Deleeuw, H. F. Schaefer III, *Chem. Phys. Lett.* **1990**, *165*, 257–264; b) W. Carrier, W. Zheng, Y. Osamura, R. I. Kaiser, *Chem. Phys.* **2006**, *330*, 275–286.
[7] a) Y. Osamura, H. F. Schaefer III, S. K. Gray, W. H. Miller, *J. Am. Chem. Soc.* **1981**, *103*, 1904–1907; b) T. J. Lee, W. D. Allen, H. F. Schaefer III, *J. Chem. Phys.* **1987**, *87*, 7062–7075.
[8] H. Leclercq, I. Dubois, *J. Mol. Spectrosc.* **1979**, *76*, 39–54.
[9] a) M. Izuha, S. Yamamoto, S. Saito, *J. Chem. Phys.* **1996**, *105*, 4923–4926; b) W. W. Harper, E. A. Ferrall, R. K. Hilliard, S. M. Stogner, R. S. Grev, D. J. Clouthier, *J. Am. Chem. Soc.* **1997**, *119*, 8361–8362; c) W. W. Harper, K. W. Waddell, D. J. Clouthier, *J. Chem. Phys.* **1997**, *107*, 8829–8839; d) T. C. Smith, H. Li, D. J. Clouthier, *J. Chem. Phys.* **2001**, *114*, 9012–9019; e) T. C. Smith, C. J. Evans, D. J. Clouthier, *J. Chem. Phys.* **2003**, *118*, 1642–1648.
[10] I.-C. Lu, W.-K. Chen, W.-J. Huang, S.-H. Lee, *J. Chem. Phys.* **2008**, *129*, 164304.
[11] a) D. A. Hostutler, T. C. Smith, H. Li, D. J. Clouthier, *J. Chem. Phys.* **1999**, *111*, 950–958; b) D. A. Hostutler, D. J. Clouthier, S. W. Pauls, *J. Chem. Phys.* **2002**, *116*, 1417–1423; c) S.-G. He, B. S. Tackett, D. J. Clouthier, *J. Chem. Phys.* **2004**, *121*, 257–264.
[12] J. M. Galbraith, H. F. Schaefer III, *J. Mol. Struct. (THEOCHEM* **1998**, *424*, 7–20.
[13] a) A. M. Thomas, B. B. Dangi, T. Yang, G. R. Tarczay, R. I. Kaiser, B.-J. Sun, S.-Y. Chen, A. H. Chang, T. L. Nguyen, J. F. Stanton, *J. Phys. Chem. Lett.* **2019**, *10*, 1264–1271; b) V. S. Krasnoukhov, V. N. Azyazov, A. M. Mebel, S. Doddipatla, Z. Yang, S. Goettl, R. I. Kaiser, *ChemPhysChem* **2021**, *22*, 1497–1504.
[14] a) M. Bogey, H. Bolvin, C. Demuynck, J. L. Destombes, *Phys. Rev. Lett.* **1991**, *66*, 413; b) G. Maier, H. P. Reisenauer, J. Glatthaar, *Chem. Eur. J.* **2002**, *8*, 4383–4391; c) L. Andrews, X. Wang, *J. Phys. Chem. A* **2002**, *106*, 7696–7702; d) M. Bogey, H. Bolvin, M. Cordonnier, C. Demuynck, J. L. Destombes, A. G. Csaszar, *J. Chem. Phys.* **1994**, *100*, 8614–8624.
[15] a) M. Cordonnier, M. Bogey, C. Demuynck, J. L. Destombes, *J. Chem. Phys.* **1992**, *97*, 7984–7989; b) M. C. McCarthy, P. Thaddeus, *J. Mol. Spectrosc.* **2003**, *222*, 248–254.
[16] a) X. Wang, L. Andrews, G. P. Kushto, *J. Phys. Chem. A* **2002**, *106*, 5809–5816; b) W. Carrier, Y. Osamura, W. Zheng, R. I. Kaiser, *Astrophys. J.* **2007**, *654*, 687.
[17] A. Ricca, C. W. Bauschlicher, *J. Phys. Chem. A* **1999**, *103*, 11121–11125.
[18] R. D. Levine, *Molecular Reaction Dynamics*, Cambridge University Press, **2005**.
[19] X. Gu, Y. Guo, F. Zhang, A. M. Mebel, R. I. Kaiser, *Faraday Discuss.* **2006**, *133*, 245–275.
[20] W. B. Miller, S. A. Safron, D. R. Herschbach, *Discuss. Faraday Soc.* **1967**, *44*, 108–122.
[21] D. S. N. Parker, F. Zhang, Y. S. Kim, R. I. Kaiser, A. Landera, V. V. Kislov, A. M. Mebel, A. G. G. M. Tielens, *Proc. Natl. Acad. Sci. USA* **2012**, *109*, 53–58.
[22] G.-S. Kim, T. L. Nguyen, A. M. Mebel, S. H. Lin, M. T. Nguyen, *J. Phys. Chem. A* **2003**, *107*, 1788–1796.
[23] a) R. I. Kaiser, P. Maksyutenko, C. Ennis, F. Zhang, X. Gu, S. P. Krishtal, A. M. Mebel, O. Kostko, M. Ahmed, *Faraday Discuss.* **2010**, *147*, 429–478; b) F. Stahl, P. Schleyer, H. Schaefer Iii, R. Kaiser, *Planet. Space Sci.* **2002**, *50*, 685–692; c) N. Balucani, A. M. Mebel, Y. T. Lee, R. I. Kaiser, *J. Phys. Chem. A* **2001**, *105*, 9813–9818; d) X. Gu, Y. Guo, E. Kawamura, R. I. Kaiser, *J. Vac. Sci. Technol. A* **2006**, *24*, 505–511; e) R. I. Kaiser, N. Balucani, D. O. Charkin, A. M. Mebel, *Chem. Phys. Lett.* **2003**, *382*, 112–119; f) Y. Guo, X. Gu, E. Kawamura, R. I. Kaiser, *Rev. Sci. Instrum.* **2006**, *77*, 034701.
[24] J. E. Sansonetti, W. C. Martin, *J. Phys. Chem. Ref. Data* **2005**, *34*, 1559–2259.
[25] a) M. F. Vernon, *PhD Dissertation*, University of California, Berkeley, **1983**; b) P. S. Weiss, *PhD Dissertation*, University of California, Berkeley, **1986**.
[26] A. M. Mebel, R. I. Kaiser, *Int. Rev. Phys. Chem.* **2015**, *34*, 461–514.
[27] a) G. D. Purvis III, R. J. Bartlett, *J. Chem. Phys.* **1982**, *76*, 1910–1918; b) C. Hampel, K. A. Peterson, H.-J. Werner, *Chem. Phys. Lett.* **1992**, *190*, 1–12; c) P. J. Knowles, C. Hampel, H. J. Werner, *J. Chem. Phys.* **1993**, *99*, 5219–5227; d) M. J. O. Deegan, P. J. Knowles, *Chem. Phys. Lett.* **1994**, *227*, 321–326.
[28] K. A. Peterson, D. E. Woon, T. H. Dunning Jr., *J. Chem. Phys.* **1994**, *100*, 7410–7415.
[29] K. A. Peterson, T. H. Dunning Jr., *J. Phys. Chem.* **1995**, *99*, 3898–3901.
[30] a) H. J. Werner, P. J. Knowles, G. Knizia, F. R. Manby, M. Schütz, P. Celani, T. Korona, R. Lindh, A. Mitrushenkov, G. Rauhut, *MOLPRO, version 2010.1, package of ab initio programs*, Cardiff University, Cardiff, **2010**.
[31] M. J. Frish, G. W. Trucks, H. B. Schlegel, G. E. Scuseria, M. A. Robb, J. R. Cheeseman, G. Scalmani, V. Barone, G. A. Petersson, H. Nakatsuji, *Gaussian 16, Revision C. 01; Gaussian*, Inc.: Wallingford, CT, **2019**.
[32] A. H. H. Chang, A. M. Mebel, X.-M. Yang, S. H. Lin, Y. T. Lee, *J. Chem. Phys.* **1998**, *109*, 2748–2761.
[33] H. Eyring, S. H. Lin, S. M. Lin, *Basic chemical kinetics*, John Wiley & Sons, New York, **1980**.
[34] a) W. L. Hase, *Acc. Chem. Res.* **1983**, *16*, 258–264; b) R. A. Marcus, *Chem. Phys. Lett.* **1988**, *144*, 208–214; c) A. H. H. Chang, D. W. Hwang, X.-M. Yang, A. M. Mebel, S. H. Lin, Y. T. Lee, *J. Chem. Phys.* **1999**, *110*, 10810–10820.
[35] A. H. H. Chang, S. H. Lin, *Chem. Phys. Lett.* **2004**, *384*, 229–235.

Manuscript received: January 11, 2021
Accepted manuscript online: December 20, 2021
Version of record online: January 19, 2022

© 2021 Wiley-VCH GmbH